Conceptual Design and Performance of Two Chopper Spectrometers for the SNS

D. L. Abernathy
Oak Ridge National Laboratory
June 6, 2000

Prepared for the SNS Instrument Oversight Committee
SNS document IS-1.1.8.4-6033-RE-A-00

Contents

1. Introduction

On November 1, 1999 at Argonne National Laboratory, a workshop was held to consider the scientific priorities for inelastic neutron scattering instruments to be available at the beginning of operations of the Spallation Neutron Source [1]. Several categories of spectrometers were identified, including those that are already under consideration and those that were felt to be of high priority for conceptual design. A high-resolution chopper spectrometer with an elastic resolution of about 1% has already been the subject of a preliminary conceptual design presented to the Instrument Oversight Committee [2]. In addition the workshop determined a lower resolution chopper spectrometer, with $\Delta\varepsilon/E_i \sim 5\%$ and a large detector coverage, should be given priority consideration. The purpose of this study to explore how two instruments meeting these user requirements can be designed for the SNS.

The primary focus of the optimization presented here will be the flux of neutrons on the sample assuming a given elastic energy resolution. By using an analytical expression for the resolution, a wide range of spectrometer configurations can be explored. It has been observed that in general, with no other constraints imposed, the flux on the sample for a given energy transfer resolution can always be improved by increasing the sample to detector distance [2-4]. When geometric constraints are applied, such as the necessity to remain outside the target monolith and avoid interferences with other beamlines and target building walls, there can be cases where a preferred length is found. However, in general, other constraints will have to be employed to guide the design process.

Section 2 explores the process of optimizing chopper spectrometers subject both to the performance constraints desired as well as the geometric constraints imposed by the SNS target building and instruments. Given the general layout determined in this way, a description of the two spectrometers and their performance is presented in Section 3, along with cost estimates and comparison to current instruments. After the conclusions in Section 4, the analytical model used to calculate the chopper spectrometer performance is given in the Appendix.

2. Optimizing flux with constraints

There are several common features of the high-resolution and high-flux spectrometers under consideration. Both operate in the thermal to epithermal energy range, with the incident neutron energy E_i between roughly 5 meV and 2 eV being selected by phasing a fast magnetic-bearing Fermi chopper with respect to the neutron production in the moderator. Both would like the maximum possible Q range with continuous coverage to large scattering angles. These considerations suggest that the best positions for chopper spectrometers at the SNS will be viewing the bottom upstream moderator, which will be decoupled and poisoned. Depending on the details of ongoing studies, this will be either an ambient water or a composite moderator. Since the chopper spectrometers will need room for detectors to the sides, the end positions are best. These are designated BL 18 and BL 9 on the target building layout shown in Figure 1.

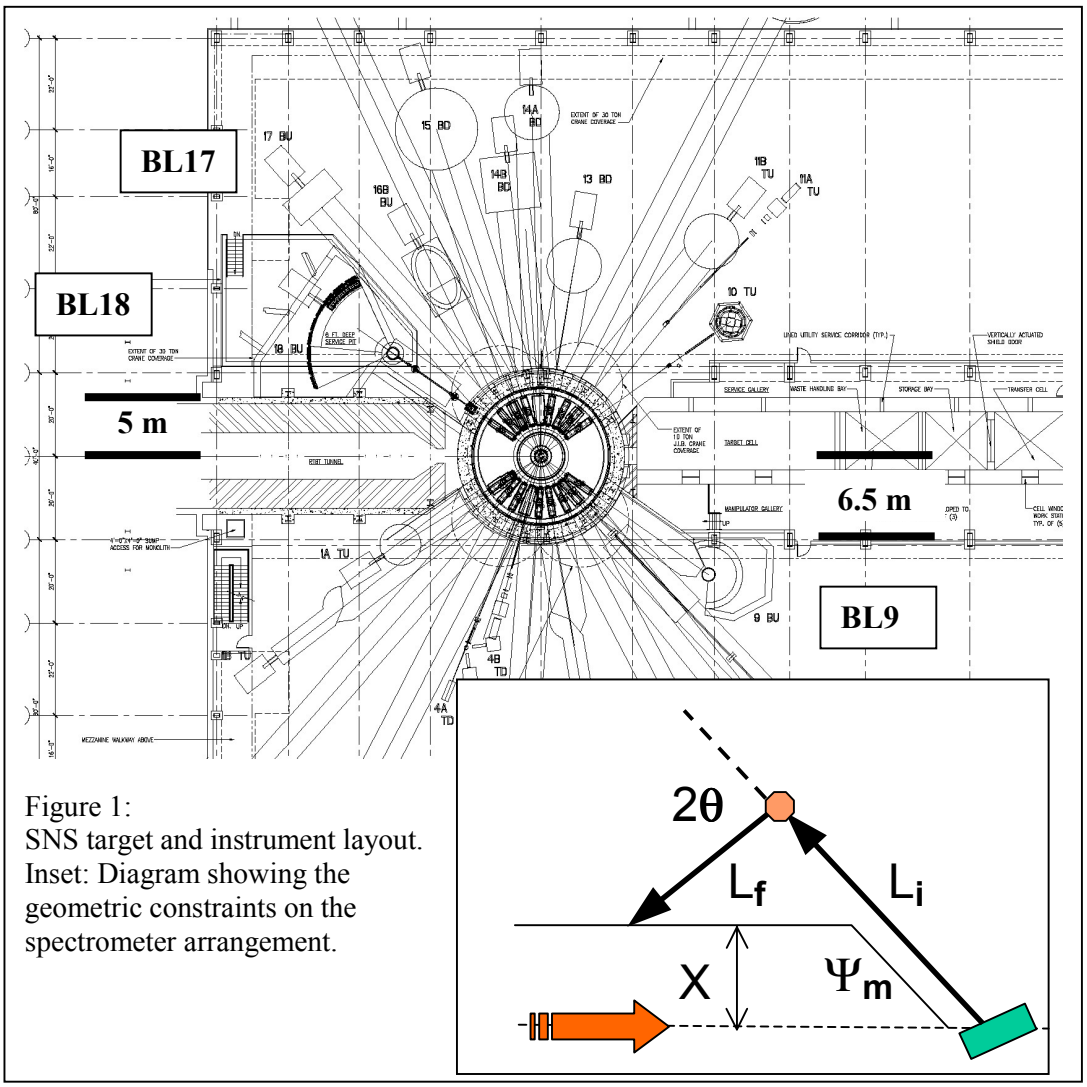

Figure 1:
SNS target and instrument layout.
Inset: Diagram showing the geometric constraints on the spectrometer arrangement.

The most obvious figure of merit for optimizing a chopper spectrometer is the flux of neutrons on the sample given a desired energy resolution. Other performance requirements, such as the **Q** resolution, could also become important, but they can often be satisfied after the general size of the instrument is determined. In general, the flux can always be improved by decreasing the chopper-to-sample distance L_2 and increasing the sample-to-detector distance L_3 (see Figure A1 and Appendix B of reference 2 for parameter definitions and discussion). Practical constraints must come into play to determine these distances. The minimum scattering angle achievable for the spectrometer will be determined by L_2. For this study it is assumed that L_2 = 1.5m for the high-flux instrument and L_2 = 2.0m for the high-resolution one.

The limits for L_3 are determined by the geometry around the instrument beamline. At the end positions the constraint is a wall running parallel to the centerline of the target building separated from it by some distance *X*, as diagrammed in the inset of Figure 1. For beamline 18, the wall is the shielding for the proton transport line and $X \sim$ 5m. The target handling area is adjacent to beamline 9, and *X* increases to approximately 6.5m there. Given the angle of the beamline Ψ_m, and the maximum scattering angle 2θ

desired, the incident flightpath length L_i and final flightpath L_f for a spectrometer configuration to be just achievable are related by

$$X = L_i \sin\psi_m - L_f \sin(2\theta - \psi_m). \quad (1)$$

If $2\theta > \Psi_m + 90°$, then 2θ is replaced by $\Psi_m + 90°$ in equation 1 since the detector locus has its maximum excursion for that value. The extreme values defined by equation 1 are a line in the space of spectrometer configurations, dividing the possible ones from the ones that would intersect the wall.

In order to optimize subject to these geometric constraints, it is necessary to calculate the flux on the sample for a given energy resolution. An analytic approximation to find the flux is quite useful, since it allows one to vary the conditions for calculation more easily than detailed numerical simulation via Monte Carlo or other techniques. Fortunately there are several authors who have given such results [3,4]. In particular, Toby Perring's approach using Gaussian approximations to the various contributions is appealing since the correlation between the moderator tilt and the sweep time contribution to the resolution is explicitly preserved. Details of the model are given in the Appendix. Briefly, the flux for a chopper spectrometer on the water moderator is found by calculating the properties of the Fermi chopper needed to achieve the required resolution. It is assumed that the Fermi chopper is always optimized for the given energy, and contributions from sample size and detector thickness are ignored. Also, the possible effect of neutron guides are not taken into account. For energies above ~100-200 meV there will be no significant gains from guides. Since both instruments have as part of their desired ranges the epithermal regime, it is best to optimize without assuming guides.

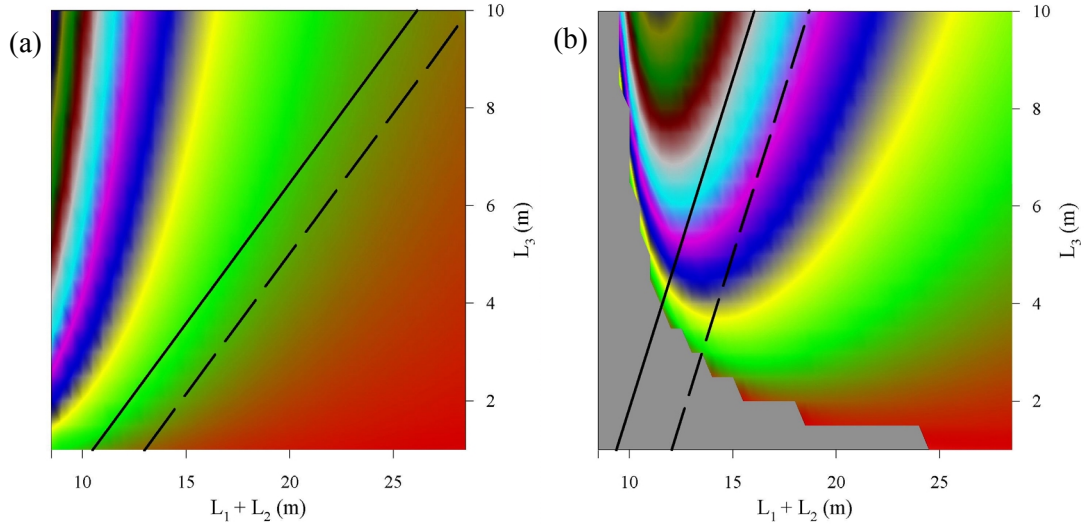

Figure 2: Color contour plots of the flux on the sample for the high flux condition $\Delta\varepsilon/E_i$ = 5% (a) and the high resolution condition ($\Delta\varepsilon/E_i$ = 1%) (b) as a function of the incident and final flighpaths. The solid and dashed lines represent geometric constraints for BL18 and BL9 respectively. See the text for range of flux values shown in each plot.

Figure 2 shows color contour plots of the flux on the sample Φ_s for the performance requirements of the two spectrometers as a function of the incident

flightpath $L_i = L_1 + L_2$ and the final flightpath $L_f = L_3$. In Figure 2a the high-flux case is shown, with an energy resolution $\Delta\varepsilon/E_i = 5\%$ FWHM for elastic scattering and L_2=1.5m. For the high-resolution case (Figure 2b), an elastic energy resolution of 1% FWHM is assumed with L_2=2.0m. In both cases the moderator parameters are the same, including the moderator tilt $\theta_m = 13.75°$. The incident energy is 200meV, but the shape of the plots is not strongly dependent on the energy and some general conclusions about the spectrometers can be drawn.

In figure 2a, the flux increases monotonically from the lower right (Φ_s = 11300 n/cm^2/s) to the upper left ($\Phi_s = 3.1\times10^6$ n/cm^2/s). For the required 5% energy resolution, the spectrometer flux cannot be optimized for any final flightpath in the range of incident flightpaths plotted. This is a consequence of the small relative size of the moderator pulse width contribution to the relaxed resolution. However, there is an optimal configuration if the geometric constraints as determined by Equation 1 are taken into account. A spectrometer at BL18 must lie below the solid line in Figure 2a, and below the dashed line for BL9. In each case it is assumed that the desired maximum 2θ is greater than 125°. Moving along this extreme, there is a broad maximum of intensity when L_3 is between 2 and 4 meters. Given the desire for ~5% energy resolution and taking into account the geometric constraints, one is led to design an instrument with a final flightpath of roughly 3m and placed as close as possible to the source.

The situation for the high-resolution spectrometer shown in Figure 2b is somewhat different. In this case there is a region (gray) in the lower left of the flux plot where the 1% energy requirement cannot be satisfied due to the length of the moderator pulse ($\Phi_s = 0$). The maximum flux plotted ($\Phi_s = 1.8\times10^5$ n/cm^2/s) occurs at L_1+L_2=11.5m and L_3=10m. At any given L_3 there is an optimum incident flightpath length in terms of the flux on the sample. Again, the solid and dashed lines correspond to the geometric constraints at BL18 and BL9, respectively, assuming for this case that the maximum desired 2θ is 60°. The optimum values of the incident flightpath move from lying within the accessible region to the excluded region as the final flightpath increases. In all cases the longer L_3 is, the more flux there is on the sample. Thus, for the high-resolution configuration L_3 must be set by another constraint. This will most likely be cost since the detector area required for a given angular coverage scales as the square of L_3.

For both cases it is evident that the geometric constraint at BL9 is more onerous than at BL18. There is also the concern that the background in the experimental hall at BL9 will be higher due to forward scattering of high energy spallation neutrons from the target. In addition, the high-resolution spectrometer is not easily accommodated at BL9 because the basement precludes easy installation of the pit needed to allow the envisioned vertical detector coverage [2]. It would be advantageous to arrange both instruments in the BL18/BL17 area, where the pit can be extended as needed and the background should be lower.

From these general considerations one is led to propose a joint optimization of the high-flux and high-resolution chopper spectrometers. Since the high-resolution instrument is naturally longer, it can take advantage of a short high-flux spectrometer on BL18 by being moved to BL17. The large angle detector back would use the space behind the other instrument. This configuration, along with the resulting performance and costs, are described in section 3.

3. Instrument parameters and performance

3.1 Spectrometer descriptions

The proposed layout for a joint installation of a high-flux and a high-resolution chopper spectrometers is shown in Figure 3. Both instruments view the bottom upstream moderator, which will either be ambient water or water-hydrogen composite. For the purposes of this discussion the source is assumed to be a decoupled water moderator with midline poisoning (24 mm). For thermal energies, this choice of poison depth will affect the minimum achievable resolution due to the wider pulseshapes. Of course there is also an increase in flux, so that an optimization of the poison depths needs to be considered.

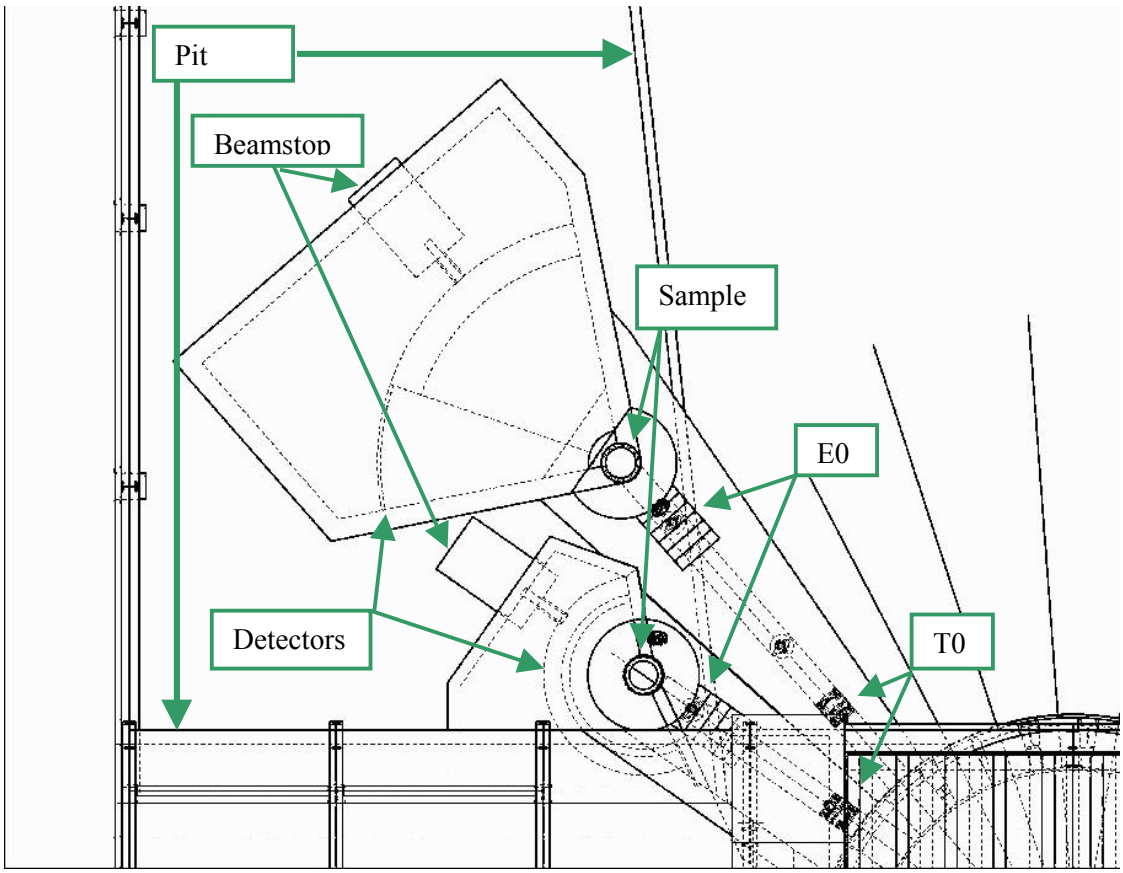

Figure 3: Layout of the high-flux (BL18) and high-resolution (BL17) chopper spectrometers.

With the standard moderator configuration, BL18 views the face at an angle of θ_m = 13.75° and BL17 is normal to the moderator. Chopper spectrometers can take advantage of the moderator tilt to improve resolution by time-focusing, so it may be possible that an alternative arrangement of the moderator would be useful. One possibility to be explored if this joint layout is used would be to make BL16 have the

normal view of the moderator, thereby increasing θ_m by 13.75° for both BL18 and BL17. It may be feasible to do this tilting only on one side of the moderator, thereby avoiding large disturbances to the target configuration and the opposite beamlines BL7-9.

As shown in Figure 3, the ~2m deep pit that was originally proposed for the high-resolution spectrometer has been extended to cover both BL18 and BL17. Although not strictly necessary for the high-flux instrument, the pit should allow for more flexibility in design. It may be possible to move the short instrument closer to the source by taking advantage of access from below for detector servicing, vacuum pump placement or other space-saving ideas.

Table 1 lists the overall characteristics of the spectrometers. The high-resolution spectrometer is similar to the preliminary design presented before [2]. The incident flightpath is now longer, in order to match the 1% energy requirement with the current model of moderator and instrument performance. The longer flightpath is also necessary to avoid the beamstop of the shorter instrument. One important issue to be addressed is the background seen in one spectrometer due to the components of the other. The most compact design is desired, subject to the need to keep background and cost at a minimum.

Figure 4 is a three-dimensional rendering of the spectrometers located in the target building. The incident beamline shielding and detector caves are translucent so

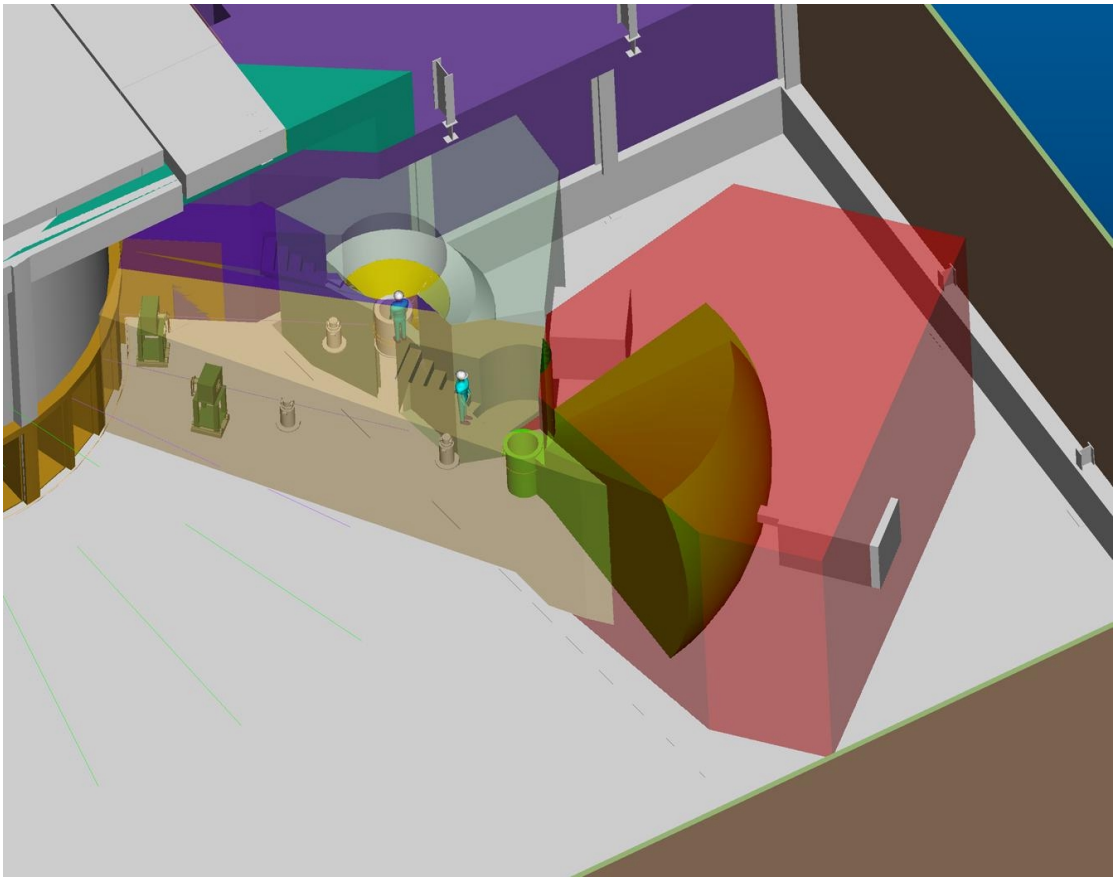

Figure 4: Three dimensional view of the two chopper spectrometers on BL18 and BL17.

that the choppers and sample positions can be seen. Such an arrangement will make a natural working area with common sample environment and other equipment needs. Preparation laboratories could be shared between the two chopper spectrometers, which should have a strong overlap in their needs. The size of the people in the figure indicate the importance of careful consideration of the shielding configuration to allow access to the spectrometer components and sample areas.

Spectrometer	High Flux	High Resolution
Moderator and dimensions	Ambient H_2O decoupled poisoned 100mm(H) x 120mm(V) Possibly composite (water-hydrogen)	
Angle	18BU: 13.75° (up to 27.5°)	17BU: 0° (up to 13.75°)
Geometry		
Source-chopper (L_1)	12.0m	15.5m
Chopper-sample (L_2)	1.5m	2m
Sample-detector (L_3)	2.5m	6m
Choppers		
T0 horizontal axis	Mechanical 60 Hz @ 7.0m	Mechanical 60 Hz @ 9.0m
T0 vertical axis	(Magnetic 300 Hz @ 7.5m)	Magnetic 300 Hz @ 10.0m
E0 (Fermi) vertical axis	Magnetic 600 Hz @ 12.0m	Magnetic 600 Hz @ 15.5m
Guide		
Type	Tapered supermirror $3\theta_c$	Tapered supermirror $3\theta_c$
Length	~7m	~11m
Apertures and collimators	2 Variable	3 Variable
After E0 (Fermi) chopper	Soller collimator	Soller collimator
Max. sample size	50mm(H) x 75mm(V)	50mm(H) x 75mm(V)
Scattering/sample chamber		
Radius sample-detector	2.5m	6m
Height	2.5m	6m
Vacuum at sample	$< 10^{-6}$ torr	$< 10^{-6}$ torr
Vacuum flightpath	$< 10^{-2}$ torr	$< 10^{-2}$ torr
Collimation	Oscillating radial collimator	Oscillating radial collimator
Shielding, inner	B_4C, 50m^2	B_4C, 150m^2
Shielding, outer	~0.5 m (TBD) thick, 100m^2	~0.5 m (TBD) thick, 400m^2
Linear PSDs		
Number	540	1200
Type	^{3}He 10 atm	^{3}He 10 atm
Diameter	25mm	25mm
Length	900mm	900mm
Resolution	25mm	25mm
Total pixels	21,600	48,000
Angular range, horizontal	-45° to -3°, 2°-150°	-30° to -2°, 2°-30° (low), 30°-60°(high)
Vertical, low bank	± 30°	± 30°
Vertical, high bank		± 10°
Low bank solid angle/area	2.15 sr / 13.5 m^2	0.70 sr / 26 m^2
High bank solid angle/area		0.12 sr / 4 m^2
Total area	13.5 m^2	30 m^2

Table 1: Instrument parameters

3.2 Resolution and flux calculations

Given the spectrometer configurations described above, we can now calculate the performance using the analytical model. Figure 5 shows the variation of intensity on the sample as the required elastic resolution is changed. Calculations are done at 50meV to represent the thermal energy regime, and 1000meV for epithermal neutrons. There are

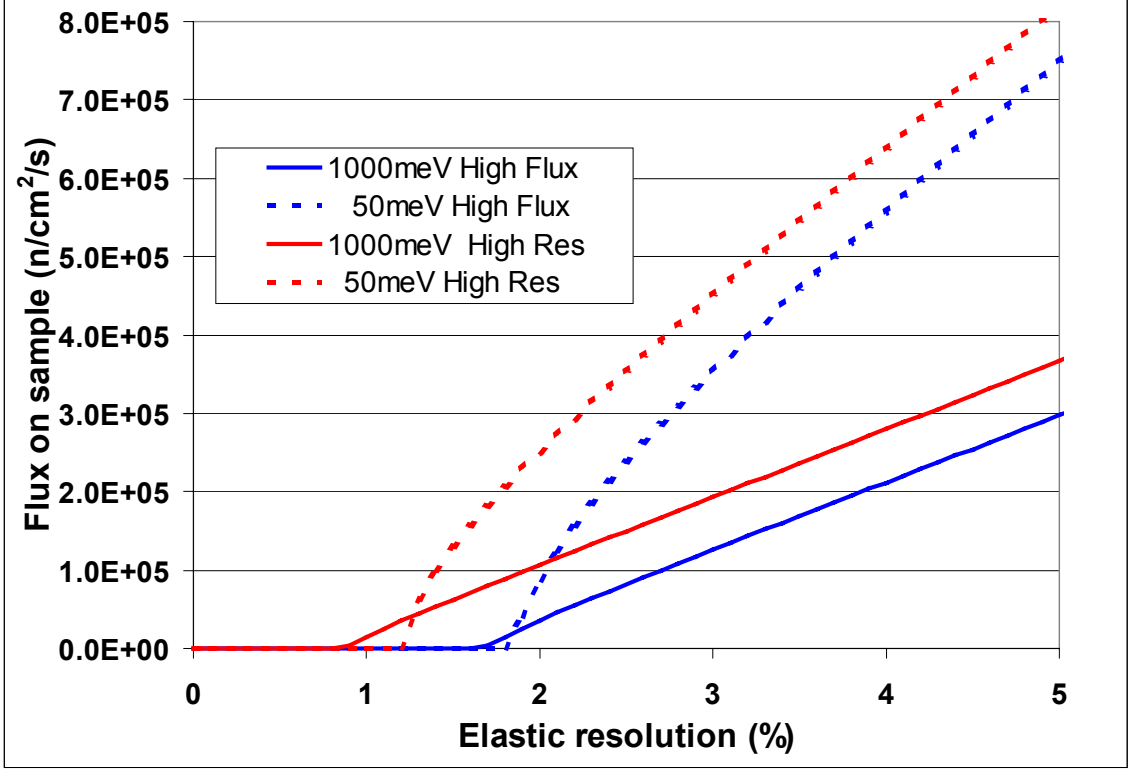

Figure 5: Flux on sample as a function of the elastic resolution for the two spectrometer configurations at 50meV and 1000meV.

several interesting points to note. Despite the names given for discussion purposes, the high resolution instrument has a larger flux on sample than the high-flux spectrometer for the same resolution. The larger final flightpath allows the incident bandwidth to be increased, thus increasing the flux. Also, although intended for use with coarse resolution, the high-flux instrument can be used with a resolution down to about 2%. This is due to the geometric constraints on placing the instrument close to the target.

Figure 6 shows the flux for the two spectrometers as a function of energy for typical resolutions of 1.4% for the high-resolution configuration and 3% for the high-flux instrument. The relatively deep poison depth of the moderator produces a flux enhancement in the thermal energy range. Although neutron guides are not explicitly calculated in this study, the lower energy part of the incident energy spectrum should be

enhanced by up to an order of magnitude if the experiment can tolerate the increased divergence.

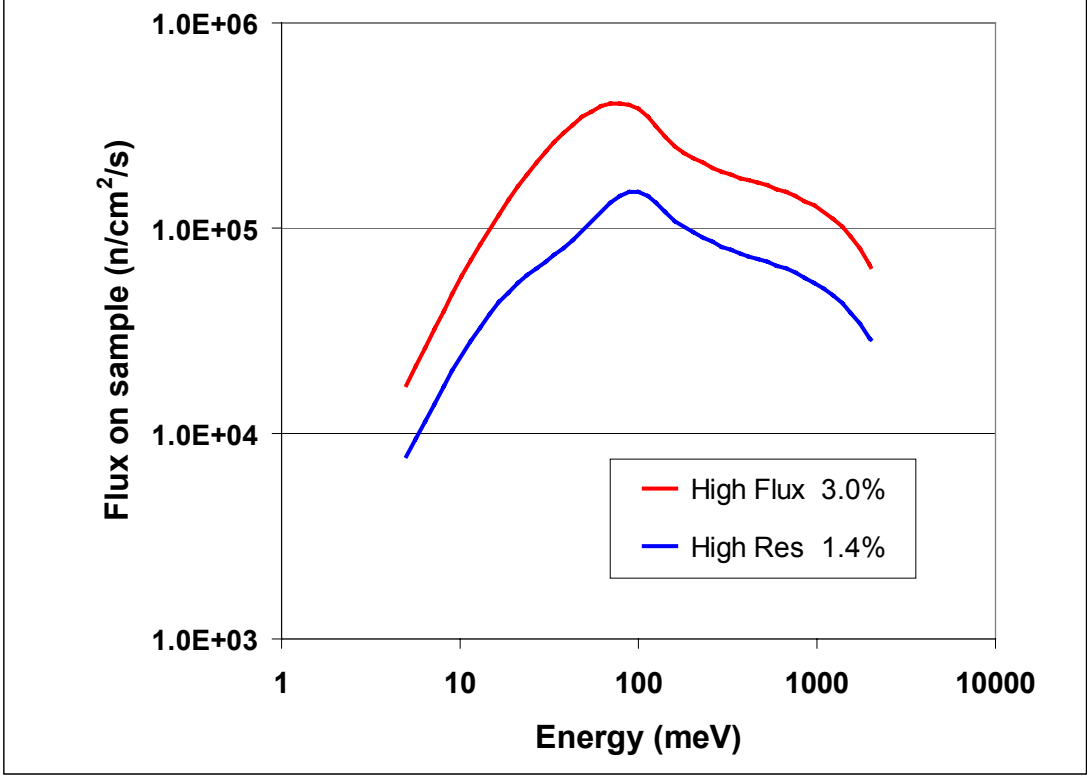

Figure 6: Flux as a function of incident energy for the high-flux configuration (3.0% elastic resolution) and the high-resolution instrument (1.4%).

As an additional measure of the performance of the two choppers, the ranges in energy transfer ω and momentum transfer Q are displayed in Figure 7. It is assumed that the incident energy range for both spectrometers is 5 – 2000 meV. The minimum energy transfer possible is taken as equal to the elastic resolution times the incident energy, in this case $0.03E_i$ for the high-flux instrument and $0.014E_i$ for the high-resolution spectrometer. The maximum energy transfer is assumed to be $0.7E_i$. The magnitude of Q is then calculated for scattering angles given in Table 1 for each instrument, and the extreme values chosen. As a point of comparison, the area covered by two other spectrometers, the high resolution backscattering spectrometer and a 10-100μeV variable resolution spectrometer, are also shown.

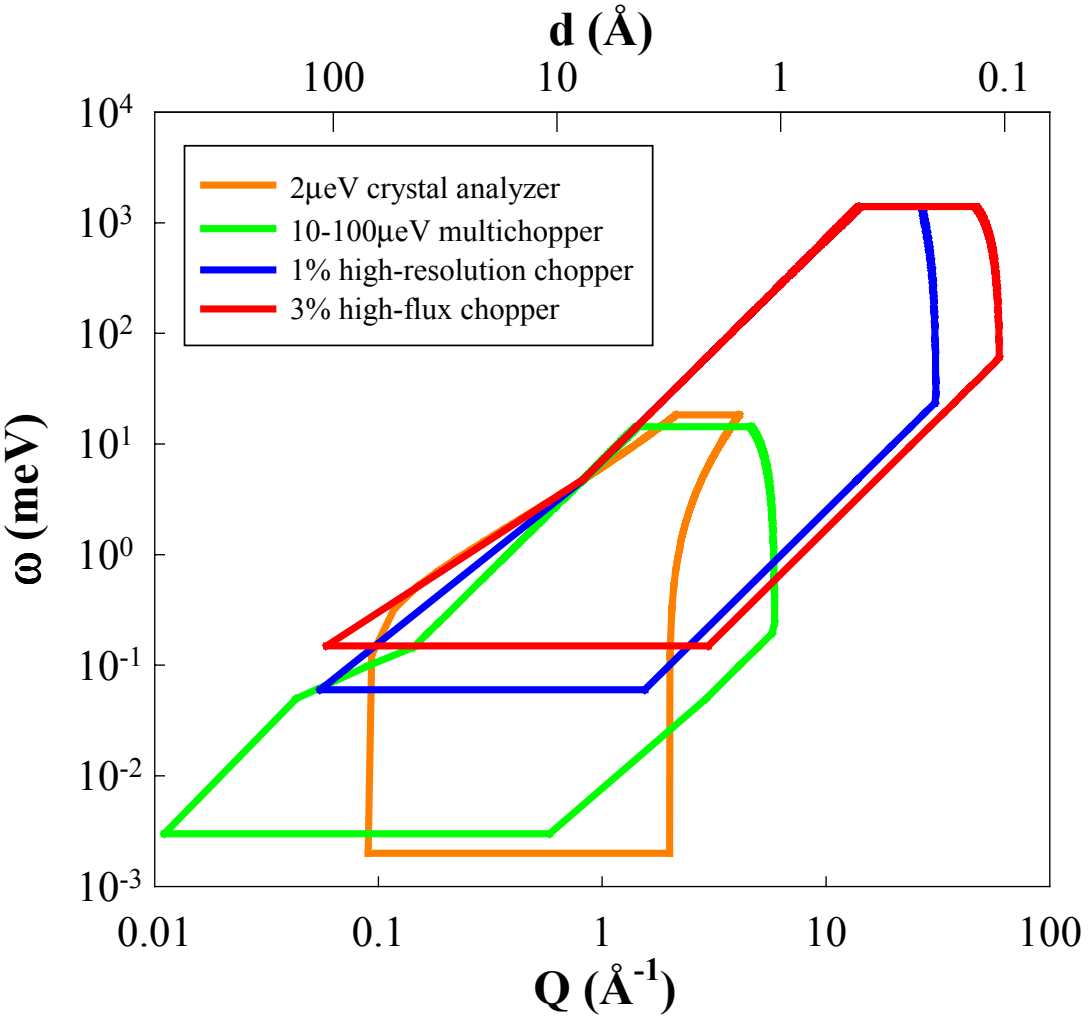

Figure 7: Areas in energy transfer-momentum transfer space covered by different inelastic scattering spectrometers under study for the SNS.

3.3 Cost estimates

It is evident that the small high-flux instrument is less expensive to build. Not only is the detector area required less than half of the high-resolution instrument, but also all shielding costs are reduced because of the smaller scattering chamber and incident flightpath. It has become apparent in the ongoing effort to estimate the cost of the SNS instruments that the beamline shielding costs are much larger than had previously been expected. Calculations indicate that roughly 2m of steel and concrete will be needed to meet the dose limits for unrestricted access in the experimental hall. For instruments as close to the target as both of the chopper spectrometers, savings from using standard shielding blocks will be minimal since each beamline's shielding merges with its neighbors' until roughly 18 – 20 m from the target. The large shielding required will pose a problem for access to beamline components as well. As a rough guess, it is

estimated that the larger, high-resolution instrument will cost ~$4 million more to construct than the smaller one.

3.4 Comparison to current chopper spectrometers

Direct geometry spectrometers using Fermi choppers are highly developed instruments for inelastic scattering at spallation neutron sources. They were among the first spectrometers to be utilized, and the understanding of their operation and optimization is well advanced. Advances in technology and scale continue, as demonstrated by the ongoing commissioning of the MAPS spectrometer at ISIS. It is therefore difficult to show orders-of-magnitude improvement in instrument performance – MAPS placed at the SNS would operate extremely well.

Instrument	L_1 (m)	L_2 (m)	L_3 (m)	Moderator, Tilt	% energy resolution	Angular Range (Hor)	Detector Solid Angle (sr)
LRMECS *ANL*	6.2	0.8	2.5	CH_4	2.5 – 7 %	3° - 120°	0.3
HRMECS *ANL*	12.7	1.1	4	CH_4	2 – 4 %	3° - 140°	0.5
HET *ISIS*	10	1.8	2.5/4	H_2O, 27°	2 – 4 %	3° - 30° 110° - 135°	0.1
MARI *ISIS*	10	1.7	4	CH_4, 13°	1 – 3 %	3° - 132°	0.1
MAPS *ISIS*	10	2	6	H_2O, 14°	1 – 3 %	3° - 60°	0.45
PHAROS *LANSCE*	18	2	4	H_2O , 15°	1.5 - 3%	1° - 140°	0.65
PHOENIX *ISIS* (HET upgrade)	12	1.8	2.5	H_2O, 27°	2 – 4 %	3° - 150°	3.1
SNS High flux	12	1.5	2.5	H_2O, 14°	2 – 4 %	3° - 150°	2.15
SNS High res.	15.5	2	6	H_2O, 0°	1 – 1.5 %	2° - 60°	0.82

Table 2: Chopper spectrometer specifications.

There are, however, several ways that the chopper spectrometers discussed in this study lead their class. Some of the operating parameters of existing and proposed instruments are listed in Table 2. Both instruments in this study will have larger detector solid angle coverage than any existing spectrometer. The entire detector arrays will be pixilated, giving great freedom in data analysis to chose the best method of grouping detectors. No current instrument uses neutron guides to enhance the flux at and below thermal energies. Provisions will be made for polarizing elements based on ^{3}He filters

so that they may be used as they are developed. Oscillating radial collimators will allow the background scattering from complex sample environments to be reduced.

4. Conclusions

This study has demonstrated that it is possible to implement two chopper spectrometers at the SNS that roughly meet the desired performance characteristics defined by a working group of inelastic scattering users. A smaller instrument, with a secondary flightpath of 2.5m and placed as close as possible to the source, will give an unprecedented range of detector angular coverage. The high flux combined with a large coverage of reciprocal space will allow studies of smaller samples, as well as routine parametric studies.

A high-resolution spectrometer can be located on the adjacent beamline, using a 6m secondary flightpath to achieve energy resolutions down to 1% of the incident energy. The detector coverage will be concentrated in the forward direction, and will also be pixilated for maximum flexibility. Both instruments will have advanced neutron guide optics for greater fluxes at thermal and lower energies. Combining both chopper spectrometers in one location, and designing them to work together, will give a coherent set of capabilities to the user community.

There is clearly need for more work on defining the optimization parameters for chopper spectrometers at the SNS. Although the intent was to make the small instrument higher in flux, this study shows that in general it will be difficult to beat the flux enhancement from a longer final flightpath because of the geometric constraints imposed by the target configuration. There are several possible paths to a more refined figure-of-merit:

1. Assume that all detected neutrons are equally valuable so that with an isotropic scatterer one would weight the flux on the sample by the detector solid angle coverage.
2. Costs could be included in the figure of merit as well – both in terms of the area of detectors that could be used as well as the length of the incident flightpath and the size of the scattering chamber and its shielding.
3. Instead of just the energy resolution the total resolution volume including **Q** could be deemed important.
4. More subtle issues such a background or range of measurement for one setting could be considered.

In all cases, the particular area of science to be addressed will influence the choice of figure-of-merit.

As a final idea, there is still the question of how to weight the advantages of having two instruments operating in roughly the same energy and **Q** range versus a single instrument that tries to cover more or less all of the user desires. Given sufficient resources a large final flightpath, large angular coverage machine could be built to include most of the characteristics desired by the different communities. What are the advantages and disadvantages of such a scheme?

References

[1] "Report on the SNS Inelastic Neutron Scattering Workshop", SNS Document number IS-1.1.8.2-8004-MM-A-00, January 31, 2000
[2] "Preliminary Conceptual Analysis for an SNS Chopper Spectrometer with 1% Energy Resolution", D. L. Abernathy, June 18, 1999, SNS Document ES-1.1.8.4-6016-RE-A-00.
[3] See for example "Pulsed Neutron Scattering", C. G. Windsor (p. 296-310).
[4] "The resolution function of a chopper spectrometer," appendix A to "High Energy Magnetic Excitations in Hexagonal Cobalt," Toby G. Perring, doctoral dissertation.

Appendix: Analytic expressions for chopper spectrometer resolution and flux

In order to explore more easily the optimization of chopper spectrometers, it is useful to have a relatively simple analytic expression for the energy resolution and flux given the geometric configuration and source characteristics. Such a model has been derived by Toby Perring of ISIS in reference 4, and is currently in use at ISIS in the program CHOP, which calculates chopper performance in order to optimize the experiments done there.

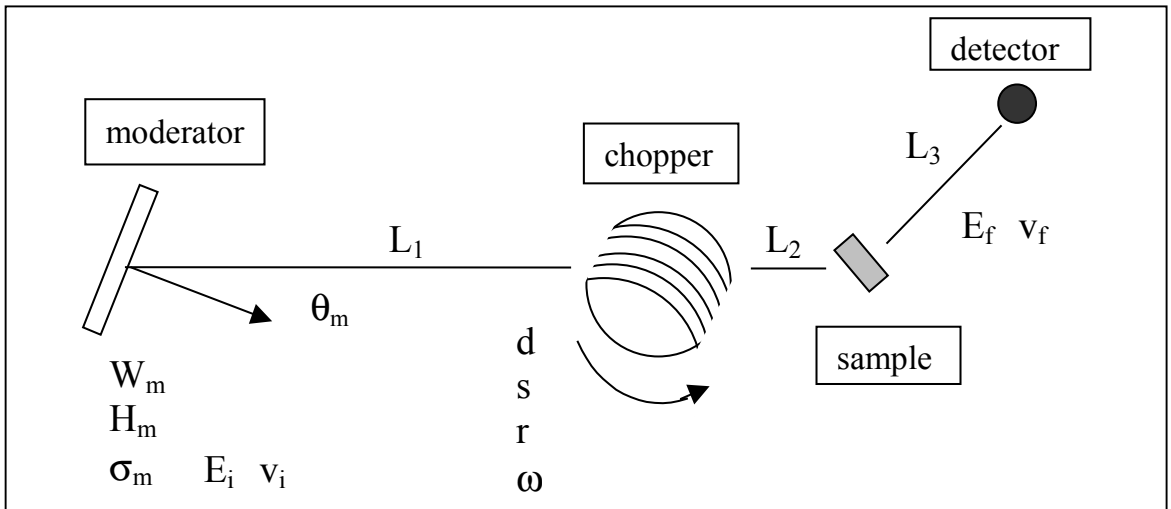

Figure A1. Schematic representation of a chopper spectrometer.

A schematic diagram for a chopper spectrometer is shown in figure A1. Geometric parameters relevant to the optimization are the moderator-chopper distance L_1, chopper-sample distance L_2, sample-detector distance L_3 . The moderator performance is characterized by its spectrum Φ as a function of neutron energy E_i or velocity v_i. Also important is the time over which neutrons are emitted, which for the present purposes is characterized by a single value σ_m. The moderator normal is inclined to the beam axis by an angle θ_m and has a width W_m and height H_m . The neutron energy is selected by a

Fermi chopper which is phased to open at time $t_1 = L_1/v_i$. The chopper transmission and open time are determined by the distance between absorbing slats d, the slat thickness s, the radius of the chopper body r, and the angular velocity ω. Neutrons scattered from the sample will have a final energy E_f or velocity v_f. The model presented here will not take into account the size or shape of the sample, the uncertainty in absorption time in the detector or the angle of scattering.

Source characteristics

The performance of the bottom upstream moderator has been calculated for the SNS assuming it to be ambient temperature water with a poison depth of 24mm (E. Iverson). Figure A2 shows the integrated flux as a function of energy. The calculations are given in units of neutrons/steradian/eV/pulse/MW, and have been scaled by the pulse rate (60 Hz), operating power (2 MW) and moderator face area (W_m x H_m = 10cm x 12cm) to give Φ in units of n/ster/cm^2/s/meV. The spectrum is well fit by the standard form that crosses over from a thermalized flux at low energies to the epithermal regime

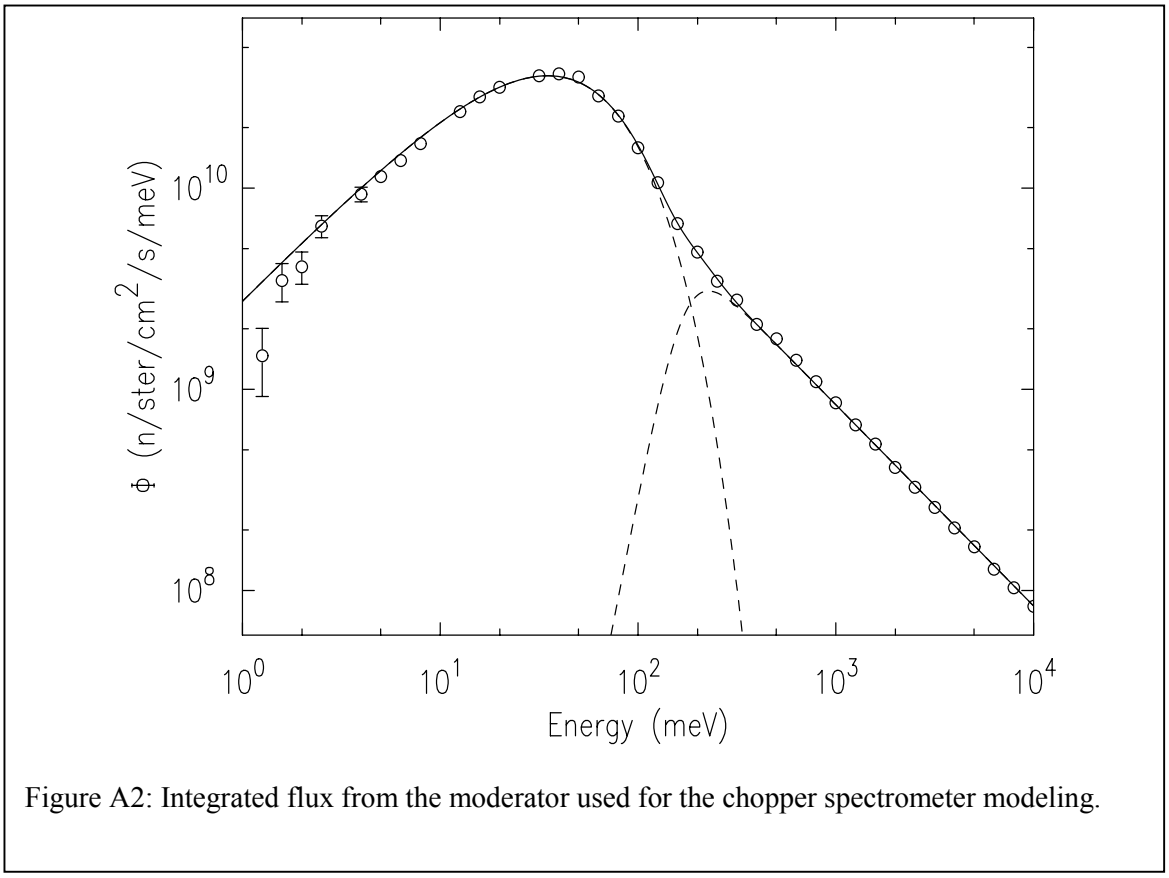

Figure A2: Integrated flux from the moderator used for the chopper spectrometer modeling.

$$\Phi(E) = \Phi_{th} \frac{E}{E_t^2} \exp\left(-\frac{E}{E_t}\right) + \Phi_{epi} \frac{\left(E/E_{ref}\right)^{\psi}}{E\left(1+\left(\frac{E_{co}}{E}\right)^{S}\right)}. \qquad \text{(A1)}$$

The fit is shown in figure A2, and the parameters are given in Table A1.

It is also necessary to characterize the pulse width from the moderator. Figure A3 plots both the root-mean-square (RMS) widths and the full-width-half-maximum (FWHM) for different energies. For the purposes of calculating the energy resolution of

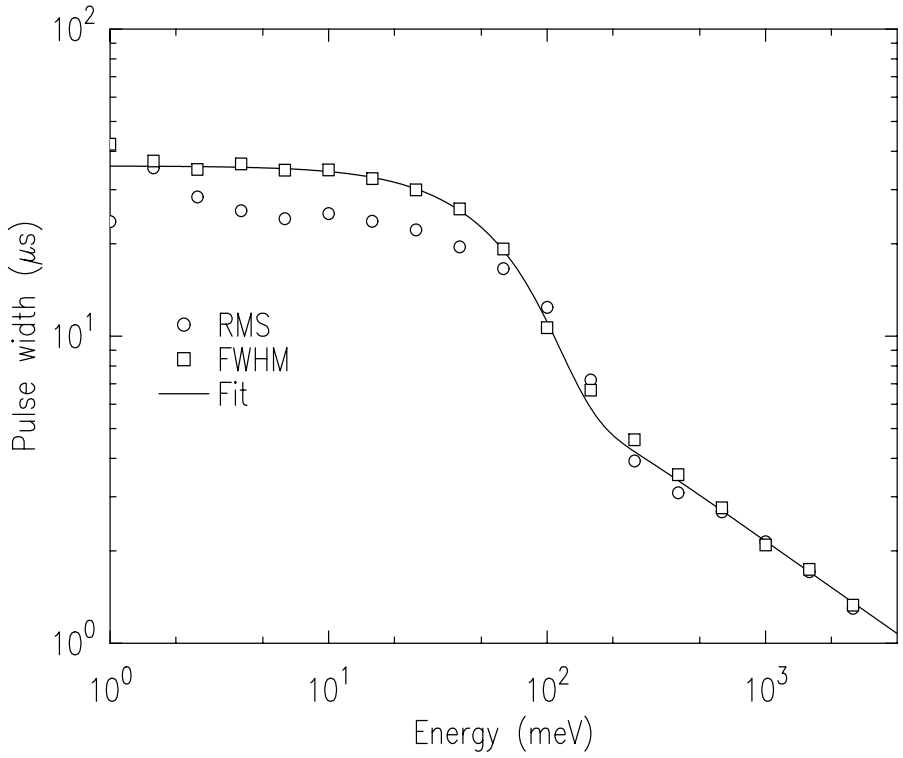

Figure A3: Pulse widths from the moderator used for the chopper spectrometer modeling.

a chopper spectrometer, we take the FWHM as the characterization of the time over which neutrons are emitted from the moderator. An empirical form describing the dependence of the FWHM on energy, inspired by equation A1 and the scaling relationship in the epithermal regime, is

$$\mathrm{FWHM}(E) = W_0 \exp\left[-(E/E_m)^{S_m}\right] + \frac{A_{epi}}{\sqrt{E}\left(1+\left(\frac{E_{epi}}{E}\right)^{S_{epi}}\right)}. \qquad \text{(A2)}$$

The parameters that define the fit shown in Figure A3 are given in Table A1.

Spectrum Φ(E) Eqn. A1		Width FWHM(E) Eqn. A2	
Φ_{th}	3.4 x 10^{12}	W_0	35.6 μs
E_t	34.9 meV	E_m	70 meV
Φ_{epi}	8.4 x 10^{11}	S_m	1.73
E_{ref}	1000 meV	A_{epi}	68 μs meV $^{1/2}$
ψ	0	E_{epi}	70 meV
E_{co}	174 meV	S_{epi}	4
S	6		

Table A1: Parameters for the source model used.

Chopper spectrometer energy resolution

The basis of the approximation to the resolution function as derived by Toby Perring [4] is to approximate all distributions by Gaussians. In this adaptation of the model, we also assume that the sample is a point and the collimation of the beamline is set so that the full face of the moderator is viewed at that point, taking into account the reduction in the width due to the moderator tilt. It is also assumed that the Fermi chopper is optimized for each energy.

The distribution in time of the neutrons passing through the chopper is triangular for an optimized slit package. The FWHM of this distribution is given by

$$\Delta_{ch} = \frac{d}{2r\omega}, \qquad \text{(A3)}$$

and the RMS width for a triangular distribution is

$$\sigma_{ch} = \frac{d}{2r\omega\sqrt{6}}. \qquad \text{(A4)}$$

The distribution of emission times is more difficult to characterize by a Gaussian since it has a tail at long times. We assume that for our purposes the Gaussian RMS value can be derived from FWHM(E) by simply scaling by the correct number for a Gaussian:

$$\sigma_m = \frac{\mathrm{FWHM}(E)}{\sqrt{8\ln 2}}. \tag{A5}$$

Studies using Monte Carlo simulation of a chopper spectrometer are underway to check this approximation against a more detailed calculation of the resolution.

Given these widths, Perring's model predicts the RMS width of the detected pulse to be

$$\begin{aligned}\sigma_T^2 = &\left(\frac{L_2}{L_1} + \left(\frac{v_i}{v_f}\right)^3 \frac{L_3}{L_1}\right)^2 \sigma_m^2 + \left(1 + \frac{L_2}{L_1} + \left(\frac{v_i}{v_f}\right)^3 \frac{L_3}{L_1}\right)^2 \sigma_{ch}^2 + \\ &\left(1 + \frac{L_2}{L_1} G + \left(\frac{v_i}{v_f}\right)^3 \frac{L_3}{L_1} G\right)^2 \frac{(W_m \cos\theta_m)^2}{12\omega^2 (L_1 + L_2)^2}\end{aligned} \tag{A6}$$

where

$$G = 1 - \frac{\omega(L_1 + L_2)\tan\theta_m}{v_i}. \tag{A7}$$

The last term in equation A6 is a moderator sweep term due to the rotating view of the moderator by the Fermi chopper. There is a correlation introduced by the moderator tilt that can cancel some or all of this contribution, giving a time focused configuration – at least for one energy and moderator tilt angle.

The FWHM energy transfer resolution is then related to this detected pulse width by

$$\frac{\Delta\varepsilon}{E_i} = 2\sqrt{8\ln 2}\left(\frac{v_f}{v_i}\right)^3 \frac{L_1}{L_3}\frac{\sigma_T}{t_1}, \tag{A8}$$

using the constant for a Gaussian to relate RMS and FWHM.

The flux at the sample position Φ_s is given approximately by

$$\begin{aligned}\Phi_s(E) &= \Phi(E)\Omega_i \beta_{ch} \left|\frac{dE}{dt}\right| \Delta_{ch} \\ &= \Phi(E)\frac{W_m \cos\theta_m H_m}{(L_1 + L_2)^2}\left(\frac{d}{d+s}\right)\frac{2v_i E_i}{L_1}\left(\frac{d}{2\omega r}\right),\end{aligned} \tag{A9}$$

where Ω_i is the solid angle incident on the sample and β_{ch} is the transmission of the Fermi chopper (in this case only taking into account the absorption of the slat). The parameters for the Fermi chopper used are s = 0.48mm, $\omega = 2\pi(600\mathrm{Hz})$, and r = 50mm. Given a desired energy resolution $\Delta\varepsilon/E_i$, E_i, E_f, moderator parameters and spectrometer geometry,

these equations define a slit spacing d to achieve that resolution. In some cases there will be no solution, if the required resolution is better than that allowed by the moderator and sweep terms. The flux is then calculated from equation A9.